Available online at www.sciencedirect.com

ScienceDirect

IFAC Papers Online CONFERENCE PAPER ARCHIVE

IFAC-PapersOnLine 49-3 (2016) 291–296

Traffic Flow Model Validation Using METANET, ADOL-C and RPROP

Adam Poole and Apostolos Kotsialos

School of Engineering and Computing Sciences, Durham University, Stockton Road, DH1 3LE, Durham, UK (e-mail: {a.j.poole, apostolos.kotsialos}@durham.ac.uk)

Abstract: Macroscopic traffic flow model calibration is an optimisation problem typically solved by a derivative-free population based stochastic search methods. This paper reports on the use of a gradient based algorithm using automatic differentiation. The ADOL-C library is coupled with the METANET source code and this system is embedded within an optimisation algorithm based on RPROP. The result is a very efficient system which is able to be calibrate METANET's second order model by determining the density and speed equation parameters as well as the fundamental diagrams used. Information obtained from the system's Jacobian provides extra insight into the system dynamics. A 22 km site is considered near Sheffield, UK and the results of a typical calibration and validation process are reported.

Keywords: Road traffic, calibration, parameter estimation, optimization, gradient methods.

1. INTRODUCTION

In Poole and Kotsialos (2012) an optimisation formulation was introduced for the macroscopic traffic flow model calibration problem which was solved by means of a genetic algorithm. The METANET Messmer and Papageorgiou (1990); Kotsialos et al. (1998, 2002) model was employed, treated as a simulation black box. An additional requirement was the automatic spatial assignment, i.e. determining the location and extension, of fundamental diagrams (FD). The motivation behind this is that current calibration practice either uses expert engineering opinion to make a decision about the FD or use a separate FD for every discrete road segment resulting from the model's discretisation rules. In the first case, intuition, past experience, visual inspection and preliminary data analysis result to an *ad-hoc* approach leading away from systems that embed knowledge in their own structure and the display of more intelligent forms of automation, Kotsialos and Poole (2013). In the latter case, overparametrisation is a clear risk since typically three parameters are necessary for defining a FD.

The problem formulation suggested in Poole and Kotsialos (2012) allows the arbitrary selection of FD location for homogeneous road stretches, which themselves are split into segments, but also penalised the variance between their parameters. The rationale behind this penalisation is that by treating the FD as an extensive quantity whose start and end are decision variables in an optimisation problem, the parameter variance penalty will result to solutions that favour similar FD. This kind of similarity was employed as guidance when validating the large scale model of the Amsterdam motorway networks, Kotsialos et al. (1998, 2002). An additional constraint imposed a maximum number of FD to be used for a site. It is left up to the optimisation algorithm to decide how many FD to be used and over which area to place them.

FD are aggregate descriptions of the infrastructure-vehicle-driver system. The variation in capacity and free speeds observed in real data are projections of the same traffic flow adapting to local inhomogeneities, e.g. drop of lanes, or different traffic composition. Variations of that system should be reflected on the FD but all FD model the same traffic flow process. This does not mean that the optimisation algorithm will equate all FD, since error minimisation is still the dominant objective.

The optimisation problem as formulated in Poole and Kotsialos (2012) is a nonlinear mixed integer optimisation problem. A genetic algorithm was used there in order to demonstrate the soundness of the approach. Based on this work, a more detailed calibration work using classic and recent variants of particle swarm optimisation (PSO) and cuckoo search algorithms was reported in Poole and Kotsialos (2016). These evolutionary algorithms were used for calibrating the Heathrow site used in Poole and Kotsialos (2012) in addition to a road stretch near Sheffield, which is considered here as well. The results reported demonstrate the validity of the approach. Optimal parameters were determined capturing the essential characteristics of the underlying traffic dynamics as was shown in the ensuing model validation, see Poole and Kotsialos (2016) for more details.

All the calibration methods used there are population based treating the METANET simulator as a simple executable invoked for each fitness function evaluation. This approach follows the common choice made regarding the optimisation algorithm used for model parameter estimation, see e.g. Spiliopoulou et al. (2014) and Ngoduy and Maher (2012). Here, a gradient based optimisation method is introduced for solving this calibration problem. Extra information that becomes available from the process of calculating partial derivatives is highlighted as well. The gradient calculation is performed by use of the automatic

2405-8963
Peer review under responsibility of International Federation of Automatic Control.
10.1016/j.ifacol.2016.07.049

differentiation algorithm ADOL-C, Walther and Griewank (2012).

Section 2 provides a brief overview of the METANET model. Section 3 outlines the optimisation problem formulation. A brief site description and overview of available data are given in section 4 and results are discussed in section 5. Section 6 concludes this paper providing the key areas of future work.

2. METANET MODEL OVERVIEW

METANET is a well known macroscopic traffic flow model. A road network is represented as a directed graph consisting of nodes and links. Links represent homogeneous road sections, where the number of lanes is a constant and there is no significant change of curvature or gradient. Nodes are connected by links and are used at places where the geometry of the motorway changes or at on-/off-ramp junctions. Traffic enters via origin links and leaves through destination links.

Time is discretised globally with a time step T and the time horizon is K steps. Each motorway link m is discretised into N_m segments of equal length L_m. The variables describing traffic conditions in segment i of link m, at time instant $t = kT$, $k = 0, 1, \ldots, K$, are the traffic density $\rho_{m,i}(k)$ (veh/km/lane) of a link m with λ_m lanes, the mean speed $v_{m,i}(k)$ (km/h) and the traffic flow $q_{m,i}(k)$ (veh/h). The discrete time motorway second order traffic flow model is the following.

$$\rho_{m,i}(k+1) = \rho_{m,i}(k) + \frac{T}{L_m\lambda_m}[q_{m,i-1}(k) - q_{m,i}(k)] \quad (1)$$

$$q_{m,i}(k) = \rho_{m,i}(k) v_{m,i}(k) \lambda_m \quad (2)$$

$$\begin{aligned} v_{m,i}(k+1) = v_{m,i}(k) &+ \frac{T}{\tau}\{V[\rho_{m,i}(k)] - v_{m,i}(k)\} \\ &+ \frac{T}{L_m} v_{m,i}(k)[v_{m,i-1}(k) - v_{m,i}(k)] \\ &- \frac{\nu T}{\tau L_m} \frac{\rho_{m,i+1}(k) - \rho_{m,i}(k)}{\rho_{m,i}(k) + \kappa} \end{aligned} \quad (3)$$

where ν and κ are speed equation parameters and $V[\rho_{m,i}(k)]$ is the FD given by

$$V[\rho_{m,i}(k)] = v_{f,m} \cdot \exp\left[-\frac{1}{\alpha_m}\left(\frac{\rho_{m,i}(k)}{\rho_{cr,m}}\right)^{\alpha_m}\right] \quad (4)$$

where $\rho_{cr,m}$ is the critical density of link m and α_m a parameter.

In order to account for speed drops due to on-ramp inflow the term $-\delta T q_\mu(k) v_{m,1}(k) / (L_m \lambda_m (\rho_{m,1}(k) + \kappa))$ is added at (3), where δ is a constant parameter, μ the merging link and m is the leaving link. This term is included only when the speed equation is applied to the first segment of the downstream link m. Speed decreases due to weaving is accounted by adding the term $-\phi T \Delta\lambda \rho_{m,N_m}(k) v_{m,N_m}(k)^2 / (L_m \lambda_m \rho_{cr,m})$ to (3), where $\Delta\lambda$ is the reduction in the number of lanes and ϕ is another parameter. Constraints are imposed in the form of a minimum speed $v_{\min}$ and a maximum density $\rho_{\max}$.

Traffic volume measurements at origins over the period of K steps are required. Speed measurements can also be used to better inform the model dynamics, but they are not necessary. In order for the speed equation to be applied at destinations s, measurements of the density trajectories $\rho_s(k)$ over the entire time horizon are provided as boundary conditions as well. For a full description of the METANET, see Messmer and Papageorgiou (1990) or its manual, METANET (2008).

3. OPTIMISATION PROBLEM FORMULATION

Equations (1)–(4) applied on an arbitrary motorway network can be expressed in the following discrete dynamic state-space system form

$$\mathbf{x}(k+1) = \mathbf{f}\left[\mathbf{x}(k), \mathbf{d}(k); \mathbf{z}\right]. \quad (5)$$

The state vector consists of the density and mean speed of every link segment, i.e.

$$\mathbf{x} = \left[\rho_{1,1}\, v_{1,1} \ldots \rho_{M_1,N_{M_1}}\, v_{M_1,N_{M_1}}\right]^T \quad (6)$$

where M_1 is the number of motorway links in the network.

The disturbance vector $\mathbf{d}$ consists of the inflows q_o entering the system from entry points (origin links) like on-ramps or the upstream main site boundary and optionally the speeds v_o at these locations; the densities ρ_s at the exit locations (destination links) like off-ramps or downstream main site boundaries; and the turning rates β_n^μ at every split node n, where μ is the main out-link. Hence,

$$\mathbf{d} = \left[q_1\, v_1 \ldots q_{M_2}\, v_{M_2} \rho_1 \ldots \rho_{M_3} \beta_1^{\mu_1} \ldots \beta_{M_4}^{\mu_{M_4}}\right]^T \quad (7)$$

where M_2 is the number of origins, M_3 the number of destinations, M_4 the number of split junctions.

$\mathbf{z} \in \mathbb{R}^\Gamma$ consists of the model parameters as encountered in the dynamic density (1), speed (3) and fundamental diagram (4) equations. It includes the network-wide global parameters of the maximum density $\rho_{\max}$, minimum speed $v_{\min}$ and the mean speed equation (3) parameters τ, ν, ϕ, δ and κ. It also contains parameters related to the fundamental diagram, i.e. v_f, α, and ρ_{cr}.

A set of measurements $\mathbf{y}$ from a number of locations along the motorway, are used for comparing reality and model output. The resulting minimisation problem is

$$\min_{\mathbf{z}} J\left[\mathbf{x}(k), \mathbf{y}(k)\right] \quad (8)$$

subject to

$$\mathbf{x}(k+1) = \mathbf{f}\left[\mathbf{x}(k), \mathbf{d}(k); \mathbf{z}\right], \mathbf{x}(0) = \mathbf{x}_0 \quad (9)$$

$$\mathbf{z}_{\min} \leq \mathbf{z} \leq \mathbf{z}_{\max} \quad (10)$$

where $J\left[\mathbf{x}(k), \mathbf{y}(k)\right]$ is a suitable error function and $\mathbf{z}_{\min}$ and $\mathbf{z}_{\max}$ are the lower and upper bounds, respectively, of $\mathbf{z}$'s elements. The evaluation of J at $\mathbf{z}$ requires the forward integration of (9) given as input the measurements of $\mathbf{x}_0$ and $\mathbf{d}(k)$.

Let $\widehat{N}$ the number of FDs used; each one's parameters ρ_{cr}, α and v_f are included in $\mathbf{z}$, i.e.

$$\mathbf{z} = \left[\tau\, \kappa\, \nu\, \rho_{\max}\, v_{\min}\, \delta\, \phi\, v_f^1\, \alpha^1\, \rho_{cr}^1 \ldots v_f^{\widehat{N}}\, \alpha^{\widehat{N}}\, \rho_{cr}^{\widehat{N}}\right]^T. \quad (11)$$

When $\widehat{N} = 1$ a single fundamental diagram is used. If $\widehat{N} = M_1$ then every link has its own FD; this is the case for

the gradient based optimisation method presented here in order to avoid integer decision variables whose derivatives are not defined.

Assume there are M_5 loop detectors at the site giving speed measurements $y_{j,v}(k)$, $j = 1, \ldots, M_5$. The measurements vector for period k $\mathbf{y}(k)$ has the form

$$\mathbf{y}(k) = \left[y_{1,v}(k) \ldots y_{M_5,v}(k)\right]^T. \tag{12}$$

Speed measurements are sufficient for the validation of a second order model by virtue of the conservation equation, as pointed out in Spiliopoulou et al. (2014).

A global list is retained assigning each sensor to the corresponding motorway link it belongs to. For each model time period k the measurement and the model outputs are compared assuming the same measurement value, since the model sample time is smaller than the sensor's.

Measurement location j's contribution to speed square error terms is given by

$$E_{j,v}\left[\mathbf{x}(k), \mathbf{y}(k)\right] = \left[y_{j,v}(k) - v_{m_j,i_j}(k)\right]^2. \tag{13}$$

The total error is given by

$$J_v\left[\mathbf{x}(k), \mathbf{y}(k)\right] = \frac{1}{KM_5} \sum_{k=1}^{K} \sum_{j=1}^{M_5} E_{j,v}\left[\mathbf{x}(k), \mathbf{y}(k)\right]. \tag{14}$$

In order to implicitly achieve the automatic assignment of similar FDs a penalty term $J_p(\mathbf{z})$ is included in the objective function.

$$J_p(\mathbf{z}) = \sum_{\ell=1}^{\widehat{N}-1} \sum_{r=\ell+1}^{\widehat{N}} \Big[w_v \left(v_f^\ell - v_f^r\right)^2 + w_\rho \left(\rho_{cr}^\ell - \rho_{cr}^r\right)^2 + w_\alpha \left(\alpha^\ell - \alpha^r\right)^2 \Big] \tag{15}$$

where w_v, w_ρ and w_α are weighting parameters set to 0.001, 0.0015 and 1.0, respectively.

The problem's objective function (8) takes the form

$$J\left[\mathbf{x}(k), \mathbf{y}(k), \mathbf{z}\right] = J_v\left[\mathbf{x}(k), \mathbf{y}(k)\right] + w_p J_p(\mathbf{z}) \tag{16}$$

where w_p a weighting parameter, which depends on the problem size; here, $w_p = 5.0$.

By iteratively substituting (9) into (8) the optimization problem can be expressed as

$$\min_{\mathbf{z}} J(\mathbf{z}) \tag{17}$$

subject to

$$\mathbf{z}_{\min} \leq \mathbf{z} \leq \mathbf{z}_{\max} \tag{18}$$

where the dependence on $\mathbf{y}(k)$ has been dropped because these are measurements that don't change. Gradient based iterative methods for solving this problem require the calculation of $\partial J/\partial \mathbf{z}$ at each iteration. From (16)

$$\frac{\partial J}{\partial \mathbf{z}} = \frac{\partial J_v(\mathbf{z})}{\partial \mathbf{z}} + \frac{\partial J_p(\mathbf{z})}{\partial \mathbf{z}}. \tag{19}$$

$\partial J_p(\mathbf{z})/\partial \mathbf{z}$ can be calculated analytically from (15) since it consists of quadratic penalty terms and therefore

$$\frac{\partial J_p(\mathbf{z})}{\partial z_\gamma} = 2 \sum_{\ell=1, \ell \neq \mathcal{Z}_\gamma}^{\widehat{N}} w_{v,\rho,\alpha} \left(z_\gamma - z_\ell\right), \gamma = 1, \ldots, \Gamma \tag{20}$$

where $\mathcal{Z}_\gamma$ is the fundamental diagram index decision variable z_γ refers to and $w_{v,\rho,\alpha}$ is given from

$$w_{v,\rho,\alpha} = \begin{cases} w_v & \text{if } z_\gamma \text{ corresponds to a free speed} \\ w_\rho & \text{if } z_\gamma \text{ corresponds to a critical density} \\ w_\alpha & \text{if } z_\gamma \text{ corresponds to an exponent} \\ 0 & \text{otherwise.} \end{cases} \tag{21}$$

From the chain rule

$$\frac{\partial J_v(\mathbf{z})}{\partial \mathbf{z}} = \frac{\partial \mathbf{x}(\mathbf{z})}{\partial \mathbf{z}}^T \frac{\partial J_v(\mathbf{z})}{\partial \mathbf{x}(\mathbf{z})}. \tag{22}$$

In view of (6) vector $\partial J_v(\mathbf{z})/\partial \mathbf{x}(\mathbf{z})$ has the form

$$\frac{\partial J_v(\mathbf{z})}{\partial \mathbf{x}(\mathbf{z})} = \left[\frac{\partial J_v(\mathbf{z})}{\partial \mathbf{x}_1(k)}^T \cdots \frac{\partial J_v(\mathbf{z})}{\partial \mathbf{x}_{M_1}(k)}^T \right]^T, \; k = 1, \ldots, K \tag{23}$$

where

$$\frac{\partial J_v(\mathbf{z})}{\partial \mathbf{x}_m(k)}^T = \left[\frac{\partial J_v(\mathbf{z})}{\partial \rho_{m,1}(k)} \frac{\partial J_v(\mathbf{z})}{\partial v_{m,1}(k)} \cdots \frac{\partial J_v(\mathbf{z})}{\partial \rho_{m,N_m}(k)} \frac{\partial J_v(\mathbf{z})}{\partial v_{m,N_m}(k)} \right]^T \quad m = 1, \ldots, M_1 \tag{24}$$

Because of the quadratic error terms (13) and the fact that J_v in (14) does not explicitly depend on the densities

$$\frac{\partial J_v(\mathbf{z})}{\partial \rho_{m,i}(k)} = 0 \text{ and} \tag{25}$$

$$\frac{\partial J_v(\mathbf{z})}{\partial v_{m,i}(k)} = \frac{2}{KM_5} \left[v_{m,i}(k) - y_{j,v}(k)\right] I_{m,i} \tag{26}$$

$$\forall\, m = 1, \ldots M_1,\; i = 1, \ldots, N_m,\; k = 1, \ldots, K$$

with $I_{m,i}$ a binary indicator function showing if there is a measurement for segment (m, i) used in the error calculation and j is the corresponding measurement station in (12).

Equations (23)–(26) allow for the analytical calculation of one factor of the right hand side of eqn. (22); in order to complete this calculation and determine its left hand side, the Jacobian matrix

$$\frac{\partial \mathbf{x}(\mathbf{z})}{\partial \mathbf{z}} = \begin{bmatrix} \frac{\partial \mathbf{x}(1)}{\partial z_1}^T & \cdots & \frac{\partial \mathbf{x}(1)}{\partial z_\Gamma}^T \\ \cdots & \cdots & \cdots \\ \frac{\partial \mathbf{x}(K)}{\partial z_1}^T & \cdots & \frac{\partial \mathbf{x}(K)}{\partial z_\Gamma}^T \end{bmatrix} \tag{27}$$

needs to be calculated, where

$$\frac{\partial \mathbf{x}(k)}{\partial z_\gamma}^T = \left[\frac{\partial \rho_{1,1}(k)}{\partial z_\gamma} \frac{\partial v_{1,1}(k)}{\partial z_\gamma} \cdots \frac{\partial \rho_{1,N_1}(k)}{\partial z_\gamma} \frac{\partial v_{1,N_1}(k)}{\partial z_\gamma} \cdots \frac{\partial \rho_{M_1,N_{M_1}}(k)}{\partial z_\gamma} \frac{\partial v_{M_1,N_{M_1}}(k)}{\partial z_\gamma} \right]^T \tag{28}$$

and because of (25) only the $\partial v_{m,i}(k)/\partial z_\gamma$ for every segment i of link m at time instant k with respect to every model parameter z_γ need to be calculated. It is exactly this quantity that the ADOL-C AD library calculates at every simulation time step. Hence, in order to obtain $\partial J(\mathbf{z})/\partial \mathbf{z}$, $\partial J_p/\partial \mathbf{z}$ and $\partial J_v/\partial \mathbf{x}$ are calculated analytically from (20) and (25)–(26), respectively, and $\partial \mathbf{x}/\partial \mathbf{z}$ is calculated by ADOL-C during a simulation run with METANET configured with $\mathbf{z}$. Having obtained this way $\partial J(\mathbf{z})/\partial \mathbf{z}$, a

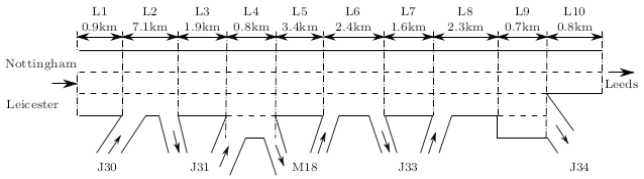

(a) Site sketch.

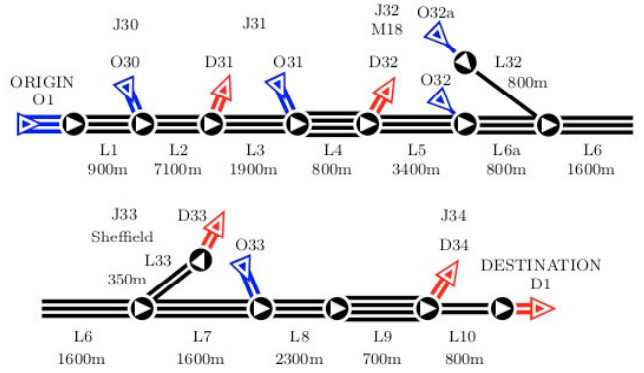

(b) METANET site representation.

Fig. 1. Sheffield site model (not on scale).

multistart version of the RPROP iterative optimisation algorithm is used in the way described in Kotsialos (2013, 2014) based on Riedmiller and Braun (1993).

A simple multistart initialisation scheme with points sampled from a Latin hypercube is sufficient.

4. SITE DESCRIPTION AND DATA USED

The test site is the Northbound M1 motorway as it enters Sheffield and can be seen in Fig. 1. It extends over 21.9 km and the METANET model consists of 20 links. Recurrent congestion has the form of a shock wave originating at the centre. Usually it occurs at the end of the link 6 where the off-ramp of Junction 33 is short and unable to cope with the demand of exiting flow. Data collected by the MIDAS system from Monday the 1st, 8th and 15th of June 2009 were used. They consist of flow, speed, and occupancy measurements per lane averaged over one minute intervals.

It is well known that $v_{m,i}$ in eqn. (2) is the space mean speed, which for a small area centred around a loop detector is estimated by the harmonic mean of individual vehicle speeds passing over the detector. The loop detectors provide arithmetic mean speeds, but assuming homogeneous traffic conditions along each lane, the harmonic and the arithmetic lane mean speeds are the same. The cross lane mean speed is estimated as the harmonic mean of the lane speed measurements,. accounting this way for the lateral speed variance but not the longitudinal.

5. RESULTS

5.1 Calibration

For the calibration optimisation problem solved, the upper and lower bounds (10) are given by Table 1. For each day of data the optimisation algorithm was repeated three times. Table 2 gives the values of total fitness function J and the corresponding error component J_v and weighted penalty $w_p J_p$.

Table 1. Traffic flow model parameters upper and lower limits.

Variable	τ	κ	ν	$v_{\min}$	$\rho_{\max}$
Max.	60	90	90	8	190
Min.	1	5	1	5	160
Variable	δ	ϕ	α_m	$v_{f,m}$	$\rho_{cr,m}$
Max.	4	3.0	5.00	130	40.0
Min.	0.001	0.00005	0.40	80	18.0

Table 2. Fitness function for three runs.

	J	J_v	$w_p J_p$
1st			
repeat 1	48.50	39.66	8.84
repeat 2	49.21	**36.96**	12.25
repeat 3	51.37	40.47	10.90
8th			
repeat 1	43.27	36.96	6.31
repeat 2	42.91	36.55	6.36
repeat 3	43.36	**36.53**	6.83
15th			
repeat 1	52.17	33.73	18.44
repeat 2	52.37	**32.13**	20.24
repeat 3	62.21	38.92	23.29

Table 3. Optimal network-wide parameter sets

	τ	κ	ν	$v_{\min}$	$\rho_{\max}$	δ	ϕ
1st	22.67	22.40	56.68	6.18	182.75	0.08	0.00005
8th	11.39	29.17	41.96	8.00	173.30	0.00008	0.00005
15th	18.57	24.71	40.34	8.00	177.83	0.093	0.00005

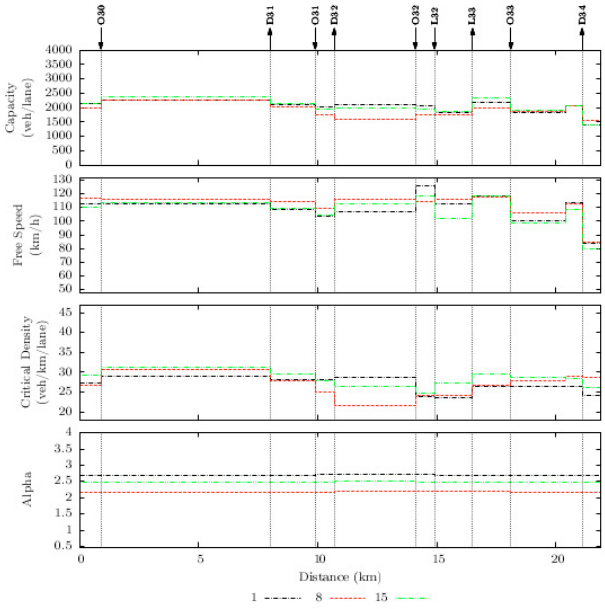

Fig. 2. Optimal FD parameters and spatial assignment.

Table 2 shows that the RPROP algorithm performs consistently for the three days and is able to find parameter sets that result to an absolute average error on the order of 6% to 7% of the speed for each detector station. Table 3 shows the network wide part of **z** from the best repeat of the three days, whereas Figure 2 depicts each link's FD parameters over space.

Figure 3 is a heatmap distance-time diagram of the speed based on data of the 15th. On the left the speed mea-

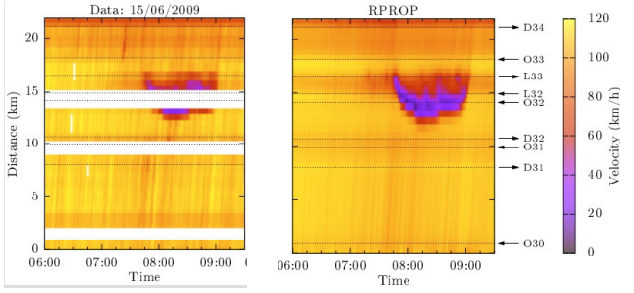

Fig. 3. Speed distance-time diagram for calibration results based on the data of the 15th.

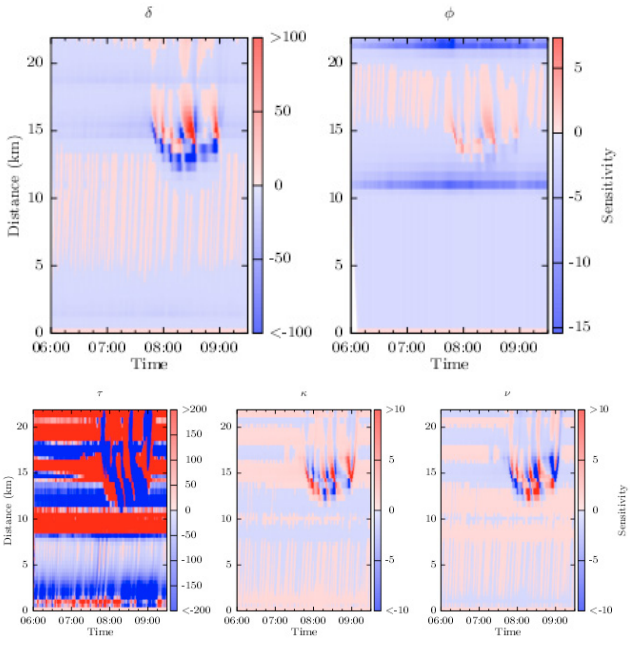

Fig. 4. Distance-time of the speed with respect to the speed equation parameters for the data of the 15th.

surements used are shown and on the right the calibrated model's output. The model is able to represent traffic dynamics and predict the congestion's spatio-temporal extension.

One of the additional benefits of calculating $\partial J/\partial \mathbf{z}$ is the calculation of the Jacobian matrix $\partial \mathbf{x}/\partial \mathbf{z}$. This provides the sensitivity of the speed at every instant and at every segment with respect to the model parameters. Figure 4 shows this sensitivity, $\partial v_{m,i}(k)/\partial z_\gamma$, γ the appropriate index for $\mathbf{z}$, for the speed equation parameters distributed over space and time for the data of the 15th. Figure 5 displays the sensitivity of the whole network's speed over space and time with respect to the FD parameters of links L1 at the start of the site, L6 at the middle, and L10 at the end.

Forwards and backwards waves are observed indicating the dominant factors affecting speed at particular point in time and space. These provide extra information regarding the flow dynamics which can be used for examining the influence of control measures or help target the most influential areas where improvements need to take place. Part of the future work is finding ways of exploiting

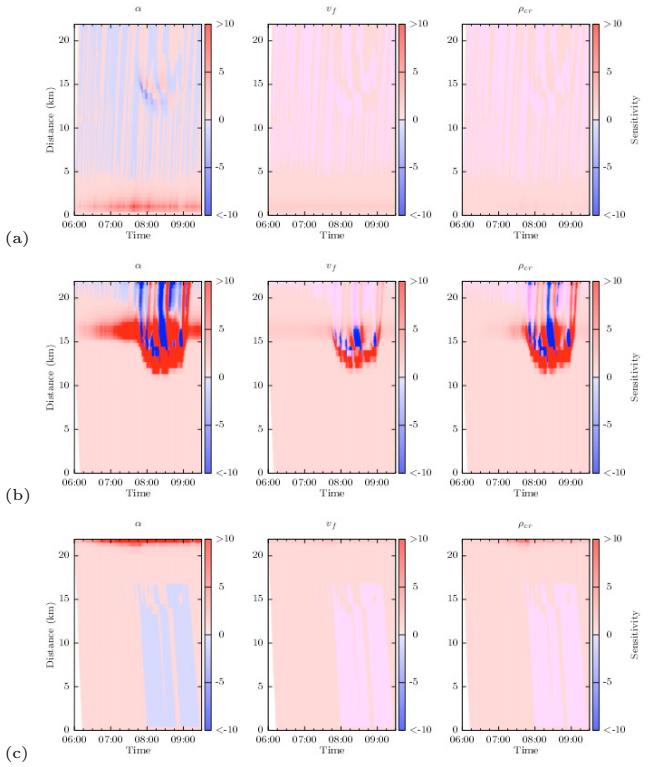

Fig. 5. Speed sensitivity over space and time with respect to the FD parameters of links (a) L1 (b) L6 (c) L10.

Table 4. Validation J_v for the solution yielding the best calibrated J_v on Table 2.

	Data from the:			
Optimal parameter set from the:	**1st**	**8th**	**15th**	**8th** (incident)
1st	36.96	141.00	106.65	55.66
8th	338.26	36.53	327.48	103.38
15th	83.22	140.47	32.13	61.65

this information for the benefit of planning systematic interventions to the traffic flow system.

5.2 Validation

The quality of the best solution obtained by the calibration process when data of a particular day were used is tested using the data of the other two days. The optimal parameter set of that day is given to METANET but the initial and boundary conditions are from the data of the other two. The model's output is then compared with the corresponding measurements from the site and J_v is calculated.

Table 4 provides the values of J_v when METANET uses the optimal parameter set $\mathbf{z}^*_{day}$ (Table 3 and Figure 2) that yields the best calibrated J_v in Table 2 (in bold). Notice that this is not always the solution with the best total fitness function value J. The diagonal elements are the calibration results and they are always smaller than the other elements of the matrix, as expected. It can be seen that $\mathbf{z}^*_{15^{th}}$ generalises better on the data of the 1st compared to $\mathbf{z}^*_{1^{st}}$ on the data of the 15th. Hence, from these two days $\mathbf{z}^*_{15^{th}}$ is preferred.

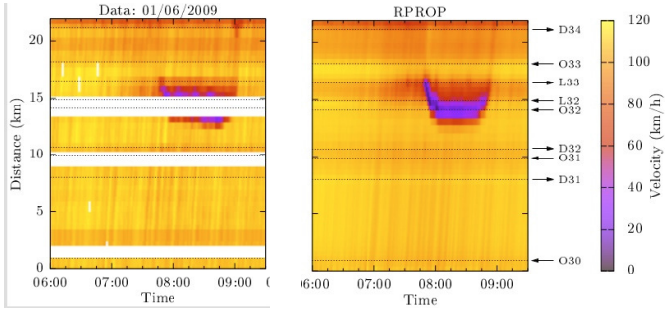

(a) data from the 1st

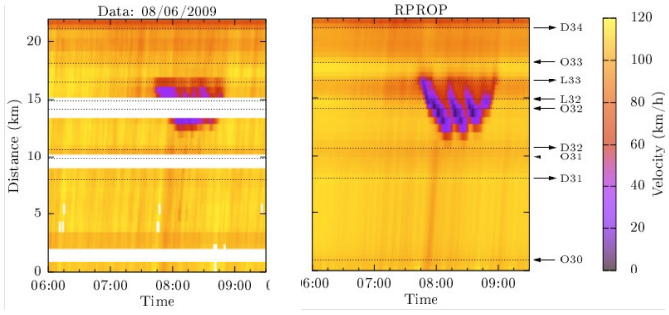

(b) data from the 8th with incident

Fig. 6. METANET simulation using $\mathbf{z}^*_{15^{th}}$.

$\mathbf{z}^*_{8^{th}}$ does not generalise well on the data of the 1st and 15th. A closer inspection of the measured speed trajectories, lead to the conclusion that on that particular day there was a sustained spill-back of congestion from destination D33. Spillbacks are particularly difficult to be captured by a macroscopic traffic flow model and distort the calibration results. However, the optimal parameter sets should remain valid even in the presence of their effects. In order to verify this, an incident was introduced for the duration of the spillback as indicated by the data at link L6, just upstream of the exit to D33. The last column of Table 4 shows the impact of introducing it. J_v for both $\mathbf{z}^*_{1^{st}}$ and $\mathbf{z}^*_{15^{th}}$ has dramatically improved. Hence, the calibrated models of the 1st and 15th remain valid for the data of the 8th. This is visualised from the distance-time diagrams shown in Figure 6. The results shown were obtained by using $\mathbf{z}^*_{15^{th}}$ for the data of the 1st and 8th with incident.

6. CONCLUSIONS AND FUTURE WORK

This paper has presented the combination of three separate methods for modelling road networks (METANET), automatic differentiation (ADOL-C) and numerical optimisation (RPROP) for developing a system of traffic flow model parameter estimation. The additional requirement of automatically selecting each FD's location and extension is not satisfied to the highest degree possible but is implicitly considered in the optimisation problem formulation. The resulting system is capable of delivering model parameter sets that remain valid under different conditions. The developed system makes use of the gradient which is calculated using the ADOL-C library. In the process of this calculation, the model's speed sensitivities with respect to the model parameters are determined. This calculation yields additional information that can be exploited for improving interventions to the traffic system. The RPROP algorithm has showed that it is capable of solving this highly complicated and demanding problem. Its simplicity of implementation has allowed the integration of the three different source codes into a single system.

A first line of research following this work will be concerned with model validation of other second order macroscopic traffic flow models that do not suffer from the isotropic assumption. Further work will also focus on improving the software implementation and RPROP's speed of convergence. Implementing integer programming methods for the problem formulation where a maximum number of used FD constraint is imposed is another important area of work. A more systematic investigation on how to use the information contained in the sensitivity distance-time diagrams for control purposes will need to be considered carefully. More detailed experiments need to be conducted in order to associate the correlation between the capacity as calculated by the calibration and the measured traffic composition.

ACKNOWLEDGEMENTS

The authors would like to thank EPSRC for partially supporting this work and the Highways Agency for providing the necessary traffic data and related information.

REFERENCES

Kotsialos, A., Pavlis, Y., Middelham, F., Diakaki, C., Vardaka, G., and Papageorgiou, M. (1998). Modelling of the large scale motorway network around amsterdam. *Preprints of the 8th IFAC Symposium on Large Scale Systems*, 2, 354–360.

Kotsialos, A. and Poole, A. (2013). Autonomic systems design for ITS applications. In *2013 16th International IEEE Conference on Intelligent Transportation Systems*, 178–183.

Kotsialos, A. (2013). Non-smooth optimization based on resilient backpropagation search for unconstrained and simply bounded problems. *Optimization Methods and Software*, 28(6), 1282–1301.

Kotsialos, A. (2014). Nonlinear optimisation using directional step lengths based on RPROP. *Optimization Letters*, 8(4), 1401–1415.

Kotsialos, A., Papageorgiou, M., Diakaki, C., Pavlis, Y., and Middelham, F. (2002). Traffic flow modeling of large-scale motorway networks using the macroscopic modeling tool METANET. *IEEE Trans. Intell. Transp. Syst.*, 3(4), 282–292.

Messmer, A. and Papageorgiou, M. (1990). METANET: A macroscopic simulation program for motorway networks. *Traffic Engineering and Control*, 31, 466–470; 549.

METANET (2008). *"METANET Documentation"*. Dynamic Systems and Simulation Laboratory, Technical University of Crete, Chania, Crete, Greece.

Ngoduy, D. and Maher, M. (2012). Calibration of second order traffic models using continuous cross entropy method. *Transportation Research Part C*, 24, 102–121.

Poole, A. and Kotsialos, A. (2016). Swarm intelligence algorithms for macroscopic traffic flow model validation with automatic assignment of fundamental diagrams. *Applied Soft Computing*, 38, 134–150.

Poole, A. and Kotsialos, A. (2012). METANET model validation using a genetic algorithm. In *Proc. of the 13th IFAC Symp. on Control in Transportation Systems*, 7–12.

Riedmiller, M. and Braun, H. (1993). A direct adaptive method for faster backpropagation learning: The rprop algorithm. In *Neural Networks, 1993., IEEE International Conference on*, 586–591. IEEE.

Spiliopoulou, A., Kontorinaki, M., Papageorgiou, M., and Kopelias, P. (2014). Macroscopic traffic flow model validation at congested freeway off-ramp areas. *Transportation Research Part C*, 41, 18–29.

Walther, A. and Griewank, A. (2012). Getting started with ADOL-C. *Combinatorial Scientific Computing*, 181–202.